JOURNAL OF AIRCRAFT
Vol. 31, No. 6, November–December 1994

Nonlinear Angle of Twist of Advanced Composite Wing Boxes Under Pure Torsion

Giulio Romeo,* Giacomo Frulla,† and Mario Busto†
Politecnico Di Torino, 10129 Turin, Italy

This article reports both the theoretical analysis and experimental results performed on advanced composite wing boxes under pure torsion. By taking into account the nonlinear effective shear modulus of skin panels operating during postbuckling, it is possible to obtain good correlation between the theoretical and the experimental behavior. An incomplete diagonal shear stress field is used to calculate the effective shear modulus that can be reduced by up to 50% in comparison to the unbuckled panels. This causes a drastic reduction in the wing box's torsional stiffness. At a shear load triple that of buckling, our results revealed angles of twist up to 50% greater than those predicted by the linear analysis.

Nomenclature

A = area enclosed by the midline of the box wall
A_{cF} = effective area of skin cooperating with flange in carrying compressive stresses parallel to flanges
A_{cU} = effective area of skin cooperating with upright in carrying compressive stresses parallel to uprights
A_{esF} = average Young's modulus of flange laminate in x direction multiplied by flange thickness (average extensional stiffness)
A_{esSx}, A_{esSy} = average Young's modulus of skin laminate in x or y direction multiplied by plate thickness
A_{esU} = average Young's modulus of upright in y direction multiplied by upright thickness
$A_{es\alpha}$ = average Young's modulus of skin laminate in α direction multiplied by plate thickness
A_F, A_U = cross-sectional area of flange and upright
A_{11i}, A_{12i}, A_{22i} = in-plane stiffnesses of ith element
A_{66DT} = laminate shear extensional stiffness in the diagonal tension field
A_{66IDT} = laminate shear extensional stiffness in the incomplete diagonal tension field
A_{66S} = shear extensional stiffness of box skin laminate
A_{66W} = shear extensional stiffness of box web laminate
a = distance between uprights
B, H = wing box width and height
E_1, E_2 = lamina modulus in longitudinal and transverse directions
G_{12} = lamina shear modulus
k = diagonal-tension factor
L = wing box length
M_t = torsion moment
N_{cF}, N_{cU} = load per unit width on effective area of skin cooperating with flanges and uprights
N_F, N_U = load per unit width on flange and upright
N_{xy} = applied shear flow
N_{xycr} = buckling shear flow of panel
N_{xyPS}, N_{xyDT} = pure shear part and diagonal tension part of the applied shear flow
N_1, N_2 = tensile and compressive load, per unit width, in wrinkles
t_F, t_U = flange and upright thickness
t_S, t_W = skin and web panel thickness
U = strain energy
α = angle of principal direction of buckle
ν_{12} = lamina major Poisson's ratio

Received Jan. 25, 1993; revision received Feb. 14, 1994; accepted for publication Feb. 28, 1994.

*Associate Professor of Design of Aerospace Structures, Department of Aerospace Engineering, Corso Duca degli Abruzzi 24.
†Aeronautical Engineer, Department of Aerospace Engineering.

Introduction

COMPOSITE aerospace structures are often designed so that they will not buckle below the limit load. Many of the analytical and experimental results available in the literature for composite panels under uniaxial compression or shear loading[1–3] report noticeable postbuckling behavior before failure. These panels are usually tested separately from the main structure, which may yield erroneous results. Additional effects are created by the structure when skin panels are in the postbuckling phase. A diagonal shear stress field[4] appears and the effective shear modulus diminishes as the stress increases. Consequently, the torsional stiffness of the whole wing box is no longer linear and is considerably reduced.

To be taken into account is the highly nonlinear behavior of specially orthotropic laminates under shear stress. The shear modulus G_{12} of these materials may vary by 50% at relatively low levels of shear stress.[5] Thus, the tangent modulus theory must be used to predict torsional behavior. For angle-ply laminates, such as those used in the present tests, the influence of the variation in G_{12} with shear stress (although taken into consideration) is not significant.

Theoretical Analysis

In a wing box of length L, width B, and height H under a pure torque M_t (Fig. 1), the angle of twist θ is defined by Bredt's theory,[4] and is extended to composite structures as

$$\theta = \frac{M_t L}{4A^2}\left(\frac{2B}{A_{66S}} + \frac{2H}{A_{66W}}\right) \tag{1}$$

Theoretically, the shear extensional stiffness of laminates is constant up to N_{xycr}; however, in practice, structures always exhibit an incomplete diagonal shear stress field in panels operating in the postbuckling phase. As is well known,[4] in

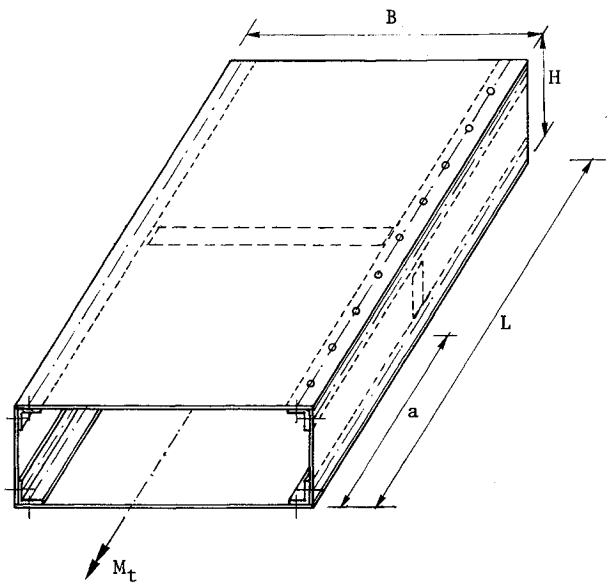

Fig. 1 Wing box structure under pure torsion.

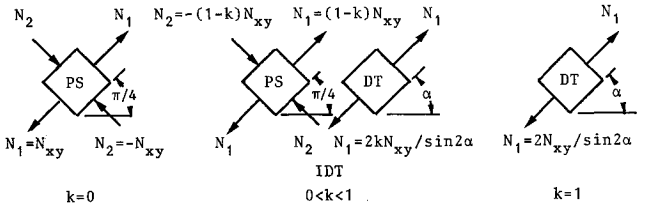

Fig. 2 State of loads, per unit width, in the skin panel for an IDT field.

this field the tension diagonal carries the majority of the shear stress, since the buckled diagonal cannot withstand any significant additional load. We therefore introduce k (characterizing the degree to which the diagonal tension is developed), defined by the empirical expression[4]

$$k = \tanh[0.5 \log(N_{xy}/N_{xycr})] \tag{2}$$

This allows N_{xy} to be divided (Fig. 2) into N_{xyPS} and N_{xyDT} by

$$N_{xy} = N_{xyPS} + N_{xyDT} \quad N_{xyDT} = kN_{xy} \quad N_{xyPS} = (1 - k)N_{xy} \tag{3}$$

A value of $k = 0$ signifies an unbuckled panel; in this case, the panel is subjected to tension and compression loads, per unit width, of the same value as the applied shear flow along two diagonals oriented at ± 45 deg, with respect to the sides. A value of $k = 1$ signifies a panel in pure diagonal tension; here the panel is subjected to a tension load $N_1 = 2N_{xy}/\sin(2\alpha)$ along one diagonal oriented at an angle α, while along the second diagonal no compression load, per unit width, is applied. In the incomplete diagonal tension (IDT), the superposition of the two load systems gives the true load system.

Determination of α

Let us consider a panel delimited by two flanges and two uprights under shear flow (Fig. 3); it has been assumed in Ref. 4 that in a controlled diagonal tension field the isotropic skin panel may also carry compressive stresses parallel to the flanges or to the uprights. According to Ref. 4, the loads per unit width in flanges, uprights (or ribs), and in the effective

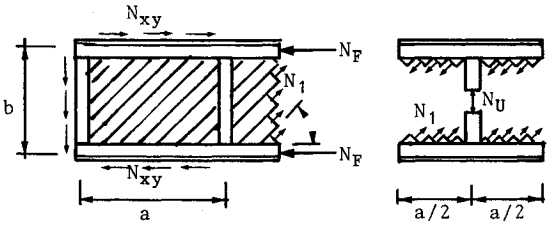

Fig. 3 State of loads, per unit width, in flanges, uprights, and in the effective panel width for a diagonal tension field.

width of the anisotropic panel cooperating with them have been determined, in the present article, respectively, as

$$N_F = -\frac{kN_{xy}b\cot(\alpha)A_{esF}}{(g_F)} \quad N_U = -\frac{kN_{xy}a\tan(\alpha)A_{esu}}{(q_U)} \tag{4}$$

$$N_{cF} = -\frac{kN_{xy}b\cot(\alpha)A_{esSx}}{(g_F)} \quad N_{cU} = -\frac{kN_{xy}a\tan(\alpha)A_{esSy}}{(q_U)} \tag{5}$$

where

$$g_F = [A_{esF}b_F + A_{esSx}0.5(1 - k)b] \qquad q_u = [A_{esU}b_U + A_{esSy}0.5(1 - k)a] \tag{6}$$

$$A_{esi} = A_{11i} - A_{12i}^2/A_{22i} \tag{7}$$

The α angle value of interest here is that which minimizes the total strain energy of the system U_{tot}

$$U_{tot} = U + U_F + U_U \tag{8}$$

$$\frac{\partial U_{tot}}{\partial \alpha} = \frac{\partial U}{\partial \alpha} + \frac{\partial U_F}{\partial \alpha} + \frac{\partial U_U}{\partial \alpha} = 0 \tag{9}$$

in which U is the strain energy of the panel in a diagonal tension field neglecting loads deriving from the pure shear field, U_F is the strain energy of the flanges and cooperating part of the panel, U_U is the strain energy of the uprights and cooperating part of the panel. The following expression of the strain energy will be used in the subsequent calculations

$$U = \frac{1}{2}\int_V \sigma\varepsilon \, dV = \frac{1}{2}[N_1^2 ab/(A_{es\alpha})] \tag{10}$$

in which

$$N_1 = \frac{kN_{xy}}{\sin(\alpha)\cos(\alpha)} \tag{11}$$

$$U_F = \frac{1}{2}\int_V \sigma_F\varepsilon_F \, dV = \frac{1}{2}\left(\frac{N_F^2 aA_F}{t_F A_{esF}} + \frac{N_{cF}^2 aA_{cF}}{t_S A_{esSx}}\right) \tag{12}$$

$$U_U = \frac{1}{2}\int_V \sigma_U\varepsilon_U \, dV = \frac{1}{2}\left(\frac{N_U^2 bA_U}{t_U A_{esU}} + \frac{N_{cU}^2 bA_{cU}}{t_S A_{esSy}}\right) \tag{13}$$

Minimizing each term of U_{tot} with respect to α, the following expressions are obtained:

$$\frac{\partial U}{\partial \alpha} = kN_{xy}ab\left(\frac{N_{xy}}{A_{es\alpha}}\frac{\sin^2\alpha - \cos^2\alpha}{\sin^3\alpha\cos^3\alpha}\right) \tag{14}$$

$$\frac{\partial U_F}{\partial \alpha} = kN_{xy}ab\left(\frac{N_F A_F}{g_F t_F} + \frac{N_{cF}A_{cF}}{g_F t_S}\right)\frac{1}{\sin^2\alpha} \tag{15}$$

$$\frac{\partial U_U}{\partial \alpha} = -kN_{xy}ab\left(\frac{N_U A_U}{q_U t_U} + \frac{N_{cU}A_{cU}}{q_U t_S}\right)\frac{1}{\cos^2\alpha} \tag{16}$$

Table 1 Panel and cross section dimensions of the first and second wing box tested under pure torsion[a]

	L	a	B	H	t_S	t_W	t_F	t_U
First wing box	720	360	396	133	2	4	4	3
Second wing box	768	384	400	135	2	4	3	2

[a]All dimensions are in millimeters.

Finally, α is obtained by assigning a stationary value to the total strain energy of the plate with respect to α [Eq. (9)], leading to

$$\tan^2\alpha = \frac{\left(\frac{kN_{xy}}{A_{es\alpha}}\frac{\sin^2\alpha - \cos^2\alpha}{\sin\alpha\cos^3\alpha}\right) + \left(\frac{N_F A_F}{g_F t_F} + \frac{N_{cF}A_{cF}}{g_F t_S}\right)}{\left(\frac{N_U A_U}{q_U t_U} + \frac{N_{cU}A_{cU}}{q_U t_S}\right)} \tag{17}$$

Since α is enclosed in both terms of Eq. (17), an iterative cycle is necessary in order to obtain the final value, which usually lies between 45–37 deg. As the angle of diagonal tension is known, it is possible to determine the extensional shear stiffness of laminate in this field, as shown below.

Determination of the Equivalent Stiffness of the Plate

The expression of the effective shear extensional stiffness of the diagonal tension anisotropic panel has been obtained by applying the principle of virtual work.

Let us consider a virtual stress system p working with an actual strain system r of the panel; the virtual work of the internal and external forces is given, after integration, by

$$\frac{N_{F_p}}{t_F}\frac{N_{F_r}A_F a}{A_{esF}} + \frac{N_{cF_p}}{t_S}\frac{N_{cF_r}A_{cF}a}{A_{esSx}} + \frac{N_{U_p}}{t_U}\frac{N_{U_r}A_U b}{A_{esU}} + \frac{N_{cU_p}}{t_S}\frac{N_{cU_r}A_{cU}b}{A_{esSy}} + \frac{N_{1_p}}{t_S}\frac{N_{1_r}abt_S}{A_{es\alpha}} - \frac{N_{xy_p}N_{xy_r}ab}{A_{66DT}} = 0 \tag{18}$$

Substituting Eqs. (4), (5), and (11), there results

$$\frac{1}{A_{66DT}} = \frac{1}{A_{es\alpha}\sin^2\alpha\cos^2\alpha} + \frac{b\cot^2\alpha}{g_F} + \frac{a\tan^2\alpha}{q_U} \tag{19}$$

In the incomplete diagonal tension field, the superposition of the two shear strain deformations [Eq. (3)] gives the true shear extensional stiffness of the panel

$$\frac{1}{A_{66IDT}} = \frac{1-k}{A_{66PS}} + \frac{k}{A_{66DT}} \tag{20}$$

It is then possible to determine the effective angle of twist θ of the wing box [Eq. (1)] for different values of the applied shear stress. By applying Eqs. (17) and (19) to the isotropic panel, the same expressions reported in Ref. 4 are obtained.

A calculation illustrating the use of this theoretical model is reported in the Appendix for one of the wing boxes tested.

Experimental Tests

Starting from the above considerations, pure torsion tests were carried out on two wing box beams with a rectangular cross section; graphite/epoxy prepreg materials (M40/914 VICOTEX) were used for manufacturing the specimens.

The first box (Fig. 4a) was manufactured in two parts, each one composed of a skin panel and two webs. They were then cured with an autoclave-controlled pressure cycle and bolted along the webs (see Table 1 for their geometrical properties).

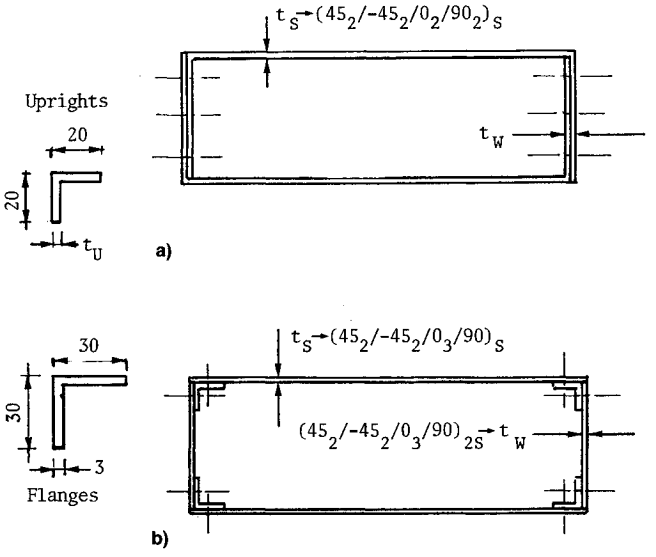

Fig. 4 Configuration and geometrical data of the wing boxes tested under torsion.

The second box (Fig. 4b) consists of four corner flanges and four panels; four L aluminium flanges were used at the corners. After the autoclave curing, the skin and web panels were bolted to the flanges along their entire length (see Table 1 for their geometrical properties).

Both specimens were initially tested without a rib bolted at the center of the wing box, and on a second occasion were tested with such a rib.

Two thin flat aluminium plates (possessing a very high in-plane stiffness and very low out-of-plane stiffness) were bolted to the ends of the boxes in order to attach them to the torsion machine (Fig. 5).[6] This is composed of a basement Ⓐ where at its four corners there are two fixed columns Ⓑ, one connecting rod Ⓒ and a hydraulic jack Ⓓ. The jack is used to apply the external load, which is then converted into a twist moment by two thick, stiff flat plates Ⓔ, to which the box's thin aluminium plates are bolted Ⓛ. The thick plates Ⓔ are connected to the frame by ball bearings Ⓕ and floating rods Ⓖ, allowing the box to be regarded as a free warping twist problem without the introduction of corrective stresses.

The twist moment was applied step-by-step; deflection data for the lower box panel were taken at different load levels by means of an electrical transducer mounted on a computer-controlled slideway. Strains were measured by several linear and rosette strain gauges placed back-to-back on both the upper and lower panels at half, a quarter and three-quarters of the length.

Material properties used in the analysis were experimentally determined to be $E_1 = 209.6$ GPa, $E_2 = 6.89$ GPa, $G_{12} = 4.26$ GPa, and $\nu_{12} = 0.305$.

The theoretical buckling load of the skin panel subjected to shear load[7,8] was determined by the computer code ALPATAR,[9] developed in our department. In this procedure, the plate equations of equilibrium, with the associated boundary conditions, were solved by the Galerkin method. A summary of the results obtained for the four tests is reported in Table 2. A very good correlation between analytical buckling loads and experimental results was obtained.

Table 2 Shear buckling analytical results of the skin panel of the two wing boxes

	First wing box		Second wing box	
	One bay	Two bay	One bay	Two bay
$N_{xy_{cr}}$, N/mm	20.5	34.2	21.01	34.19
$M_{t_{cr}}$, kNm	2.2	3.7	2.27	3.69

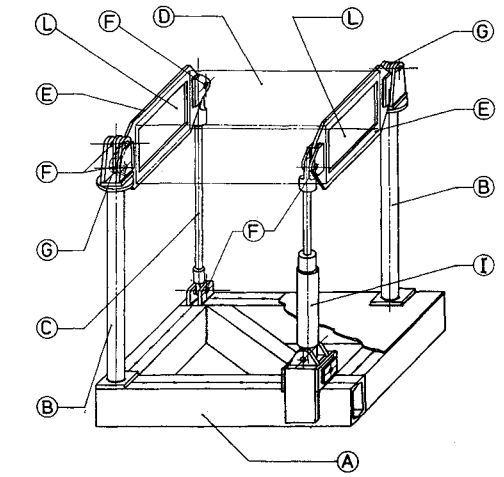

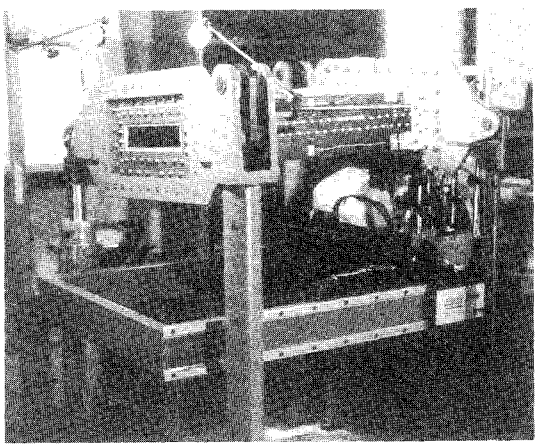

Fig. 5 Overall view of the torsion machine.

Experimental Results

The angle of twist between the bulkheads as a function of the applied torsion moment is reported in Fig. 6 for the four wing box beams. The linear behavior traced here was determined by Eq. (1), in which the shear extensional stiffnesses are considered constant; it clearly varies considerably from the experimental results. However, the influence of the variation of A_{66S} is evident, since the panel operated in an incomplete diagonal tension field. In this situation the shear stiffness [Eq. (20)] changes as a function of the shear flow, modifying considerably the torsional stiffness of the wing box. Here, a good correlation was obtained between the results determined by the present theoretical analysis and the experimental ones.

The experimental strains and deflection curves obtained from the test on the second type of wing box with the bolted rib are reported in Figs. 7 and 8. Figure 7 shows experimental strains as a function of the applied torsion moment, measured by two back-to-back rosettes placed at one-quarter length of the skin panels ($L/4$, $B/2$). The reported mean value of the two rosettes is considered to be the membrane value. Shear strain (Fig. 7a) was almost constant along the thickness, and quite linear with the moment, up to a value of 3.9 kNm. From

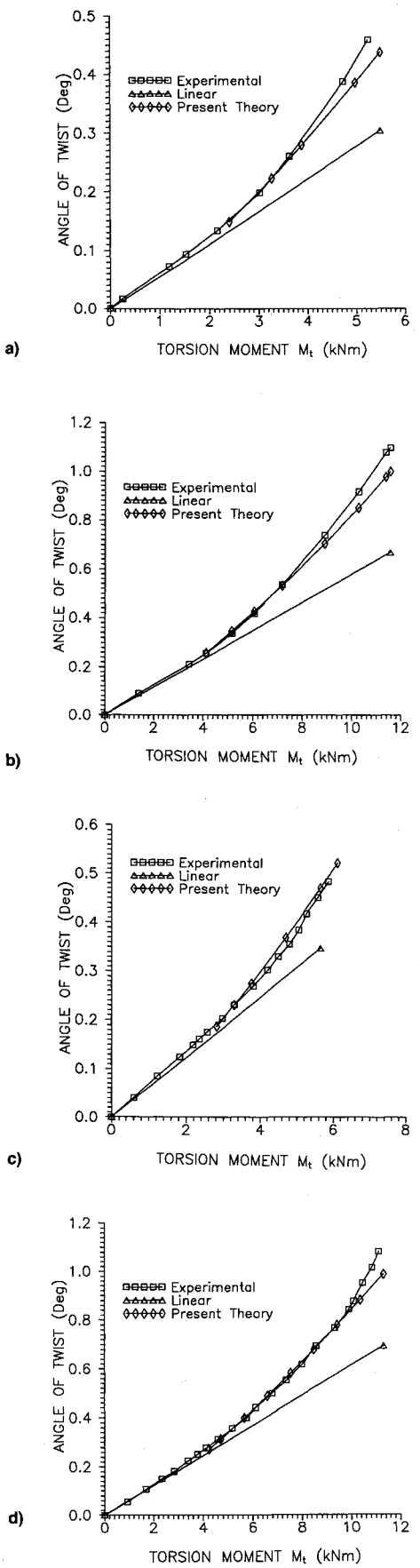

Fig. 6 Experimental and analytical θ vs M_t considering A_{66S} constant (linear) and A_{66S} variable (present theory): a) first wing box without a rib bolted at the center of the beam, b) first wing box with a rib bolted at the center of the beam, c) second wing box without a rib bolted at the center of the beam, and d) second wing box with a rib bolted at the center of the beam.

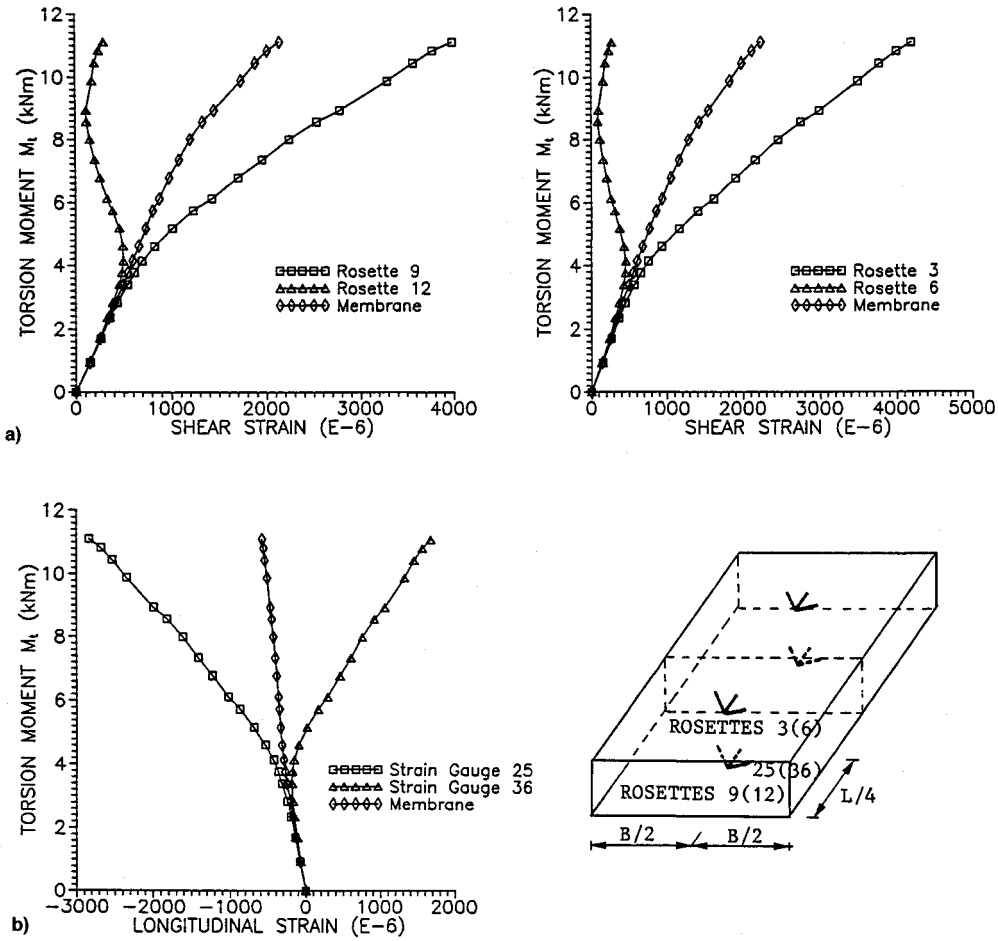

Fig. 7 Torsion moment vs experimental strains measured at one-quarter length ($L/4$, $B/2$) of the second wing box with a rib bolted at the center of the beam: a) shear strain of lower (left) and upper (right) skin panels as obtained by back-to-back rosettes and by average values (membrane) and b) back-to-back linear strain of the lower panel measured by gauges bonded at 45 deg.

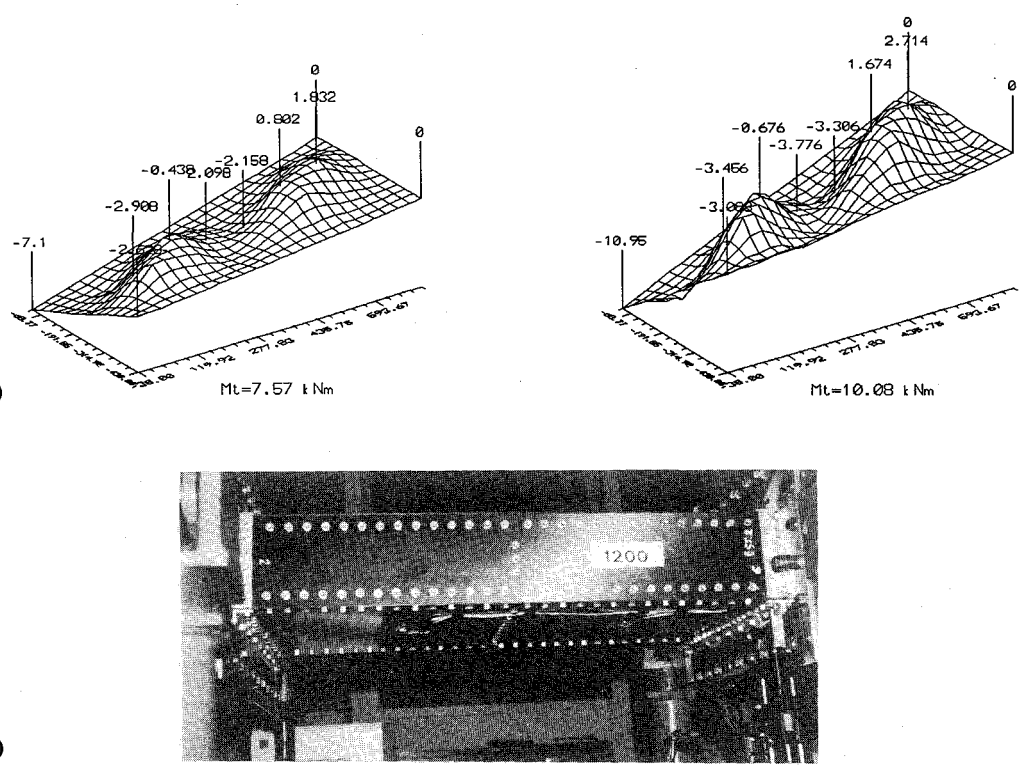

Fig. 8 Second wing box with a rib bolted at the center of the beam: a) experimental out-of-plane deflections at two values of applied twist moment and b) wing box under a twist moment of 11.3 kNm.

this point, however, we can clearly see the nonlinear behavior of membrane shear strain due to buckling. Linear strains measured by back-to-back gauges bonded on the panel at 45 deg, diagonal in compression, are reported in Fig. 7b; buckling is also evident and clearly demonstrated by a strain reversal.

Figure 8 shows the experimental deflections measured in 48 points of the lower panel, at two values of applied twist moment; one can easily detect the influence of the buckling waves on the panel's deflection.

Results very similar to those shown were obtained for the other three tests at different applied twist moment.

In the two wing boxes with the bolted rib, testing was performed up to the failure torsion moments of 12.5 and 12.2 kNm, respectively. Failure resulted in a delamination of the skin panels as a consequence of the very high deflection wave of the buckled panel. Of note is the fact that the failure load was approximately one-third that predicted by classical lamination theory applied to an unbuckled panel under in-plane shear. A nonlinear analysis is under development to study the postbuckling behaviour of anisotropic panels.[10]

Conclusions

A good correlation between theoretical analysis and experimental results was obtained for wing boxes under pure torsion by considering the effects of the nonlinear shear modulus of panels operating under an incomplete diagonal shear stress. Although it was confirmed that composite panels can operate in the postbuckling field, these tests clearly demonstrate that the buckling of panels can drastically reduce the effective torsional stiffness of the structure as a whole. Consequently, static and dynamic behavior of an entire wing may be changed, modifying the performance of aircraft.

Appendix

The calculation reported in this Appendix concerns the second wing box with a bolted rib. A computer program "CASS" has been developed in order to work out the angle of twist of a wing box with certain geometrical and mechanical parameters. The geometrical parameters introduced are a = 384, B = 400, L = 768, H = 135, t_S = 2, t_F = 3, t_U = 2, b_F = 60, and b_U = 40 mm, also, N_{xycr} = 34.2 N/mm, and N_{xy} = 39.26 N/mm corresponding to twist moment M_t = 4.24 kNm.

The mechanical parameters involve the characteristic of the panels, flanges and uprights; the skin panel in-plane stiffnesses are A_{11S} = 219,012, A_{12S} = 53,190, A_{22S} = 117,347, A_{66S} = 57,495, and $A_{es\alpha}$ = 150,713 N/mm.

The aluminium alloy flanges and upright Young's modulus is E = 71,613 MPa. The diagonal-tension factor corresponding to this applied load level is k = 0.029 [Eq. (2)]. Using Eqs. (3–7), all the parameters necessary to work out α are obtained. The iteration involving α can start from these parameters [Eq. (17)]. Subsequently the A_{66DT} stiffness [Eq. (19)] and A_{66IDT} stiffness [Eq. (20)] are obtained. Introducing all these into Eq. (1), the angle of twist θ is found out. The results for various applied load values are reported in Table A1. In the pure shear field, α should be, for an isolated panel, 45 deg; however, this value has not been rigorously obtained since the presence of flanges and uprights.

Table A1 Analytical results of the second wing box with a rib bolted at the center of the beam

M_t, kNm	N_{xy}, N/mm	K	α, deg	A_{66IDT}, N/mm	θ, deg
4.24	39.26	0.029	42.07	54,544	0.27
4.71	43.61	0.053	42.05	52,424	0.313
5.65	52.31	0.092	42.01	49,019	0.398
6.59	61.02	0.125	41.98	46,378	0.487
7.53	69.72	0.154	41.94	44,248	0.581
8.48	78.52	0.178	41.91	42,482	0.677
9.42	87.22	0.200	41.89	40,985	0.777
10.36	95.93	0.220	41.87	39,694	0.879
11.30	104.63	0.238	41.846	38,565	0.985

References

[1]Starnes, J. H., Dickson, J. N., and Rouse, M., "Postbuckling Behaviour of Graphite-Epoxy Panels," *Proceedings of ACEE Composite Structures Technology*, 1984, pp. 137–159 (NASA CP 2321); also AIAA Paper 85-0771, Pt. 1, 1985.

[2]Rouse, M., "Postbuckling of Flat Unstiffened Graphite-Epoxy Plates Loaded in Shear," *Proceedings of the AIAA/ASME/ASCE/AHS 26th Structures, Structural Dynamics, and Materials Conference* (Orlando, FL), AIAA, Washington, DC, 1985, pp. 605–616 (AIAA Paper 851).

[3]Romeo, G., and Gaetani, G., "Effect of Low Velocity Impact Damage on the Postbuckling Behaviour of Composite Panels," *Proceedings of the 17th ICAS Congress* (Stockholm, Sweden), Vol. I, AIAA, Washington, DC, 1990, pp. 994–1004.

[4]Kuhn, P., *Stresses in Aircraft and Shell Structures*, 1st ed., McGraw-Hill, New York, 1956.

[5]Garber, D. P., "Tensile Stress-Strain Behaviour of Graphite/Epoxy Laminates," NASA CR-3592, Aug. 1982.

[6]Antona, E., and Gabrielli, G., "Un'indagine Sperimentale Alari a Cassone Soggette a Torsione (Experimental Investigation of Wing Box Structures Under Pure Torsion)," *l'Aerotecnica Missili e Spazio*, No. 1, Feb. 1974, pp. 13–24 (in Italian).

[7]Whitney, J. M., "Buckling of Anisotropic Laminated Cylindrical Plates," *AIAA Journal*, Vol. 22, Nov. 1984, pp. 1641–1645.

[8]Housner, J. M., and Stein, M., "Numerical Analysis and Parametric Studies on the Buckling of Composite Orthotropic Compression and Shear Panels," NASA TN D-7996, Oct. 1975.

[9]Romeo, G., Alonso, C., and Pennavaria, A., "Buckling of Laminated Cylindrical Plates Including Effects of Shear Deformation," *Proceedings of the International Symposium on Space Application of Advanced Structural Materials*, ESA-ESTEC, ESA SP-303, Noordwijk, The Netherlands, 1990, pp. 365–370.

[10]Romeo, G., and Frulla, G., "Postbuckling Behaviour of Anisotropic Plates Under Biaxial Compression and Shear Loads," *Proceedings of the 18th ICAS Congress* (Beijing, People's Republic of China), Vol. II, AIAA, Washington, DC, 1992, pp. 1936–1944.